

1. INTRODUCTION AND MOTIVATION

Introduction

- Ionospheric F-region plasma irregularities associated with equatorial spread F (ESF) can be observed over a wide range of scale sizes.
- ESF observed after sunset and before local midnight (i.e., the post-sunset sector) is often associated with equatorial F-region conditions around dusk that favor the growth of the ionospheric Rayleigh-Taylor instability [1].
- Recent studies have focused, among other things, on a better understanding of ESF that appears outside the post-sunset sector (e.g., in the post-midnight sector).

Motivation

- A 14-panel version of the Advanced Modular Incoherent Scatter Radar (AMISR-14) has been deployed at the Jicamarca Radio Observatory (JRO). Its electronic beam-steering capability enables two-dimensional (2D) observations of the ESF irregularities [2, 3].
- We point out that the correlation of locally observed thermospheric (e.g., neutral winds) and ionospheric (e.g., vertical plasma drifts) conditions with ESF events may benefit from an explicit identification of their genesis (i.e., local or non-local).
- Here, we present and discuss results of an effort that used 2D F-region observations made by AMISR-14 to identify the genesis of post-midnight ESF events.

2. RELEVANCE

- The occurrence of post-midnight ESF and its variation with season and solar activity has been studied using conventional (i.e., single beam) radar systems [4, 5, 6].
- However, Zhan et al. [6] pointed out difficulties in using conventional radar observations to determine whether post-midnight ESF was generated near the observation site or drifted into the instrument field of view (FoV).
- Post-midnight irregularity events have been analyzed using radars with an electronic beam-steering capability only at sites outside the equatorial region [e.g., 7, 8].
- However, field-aligned irregularities at off-equatorial locations ($\sim 10^\circ$ dip latitude) must reach an apex altitude of at least ~ 400 km to be measured at ~ 200 km [7].
- The analysis in this poster expands upon previous studies by revealing, unambiguously, the local origin of post-midnight ESF events.

3. SCIENCE QUESTIONS (SQs)

- SQ1. How often are post-midnight ESF radar events observed over the JRO generated locally?
- SQ2. To what extent are the occurrence rates of local and non-local post-midnight events affected by geomagnetic and solar flux conditions?

4. EXPERIMENTAL SETUP

- AMISR-14 operates in the UHF band (i.e., 445 MHz). Measurements are thus of Bragg scattering off irregularities with a scale-size of ~ 33 cm.
- Figure 1 shows a sketch of the 10-beam AMISR-14 F-region mode. At 350 km in altitude, AMISR-14 images the ionosphere for ~ 200 km to the west and to the east of the JRO.

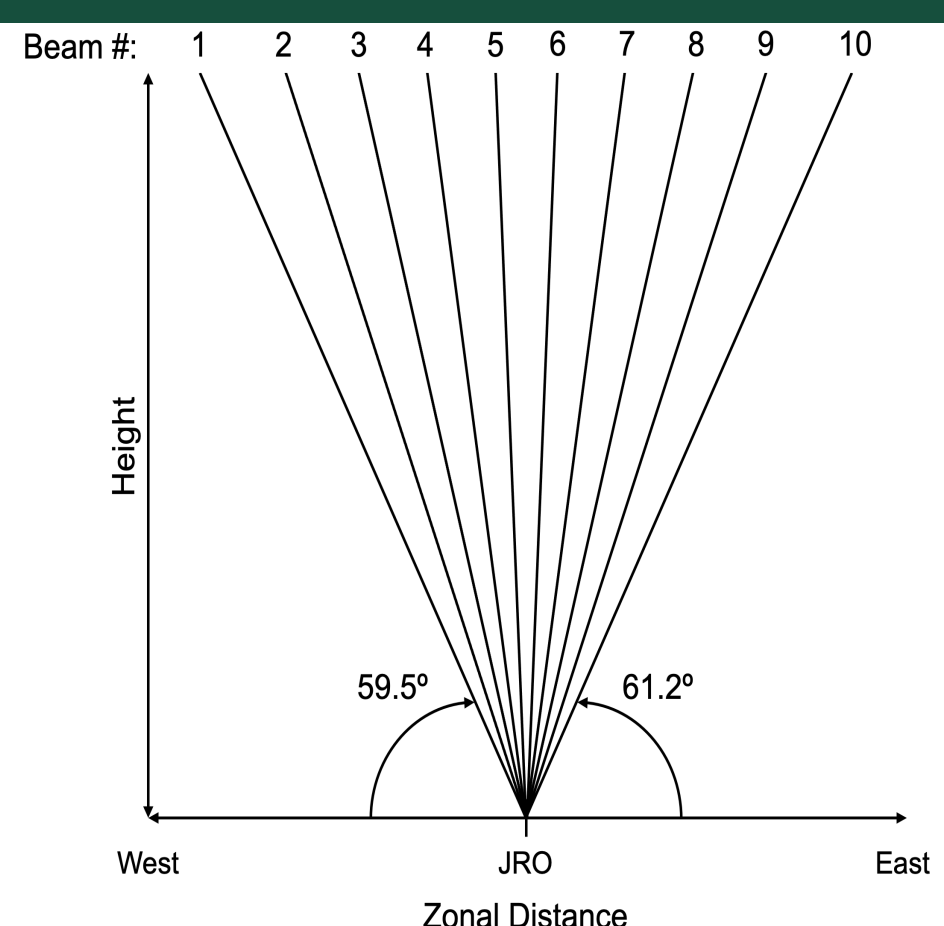


Figure 1. Sketch of the ten pointing directions in the magnetic equatorial (i.e., East-West) plane of the AMISR-14 F-region mode.

5. ANALYSIS

- 396 nights of observations made with AMISR-14 were available for analysis between July 2021 and August 2023.
- We used range-time-intensity (RTI) maps generated with AMISR-14 beams 5 and 6 to (i) identify echo events that were initially measured in the post-midnight sector, (ii) determine which post-midnight events were isolated (i.e., there were no significant echoes measured during the hour preceding the onset of post-midnight echoes), and, finally, (iii) consider only isolated post-midnight events that displayed significant vertical development (i.e., the echoes extended for at least ~ 50 km in altitude).
- We identified 51 nights with an isolated post-midnight ESF event.
- Figure 2 shows an example of the isolated post-midnight ESF event in observations made beginning on 16 September 2021. The RTI map of the vertical beam is analogous to conventional (i.e., single beam) measurements of post-midnight ESF made in the past.

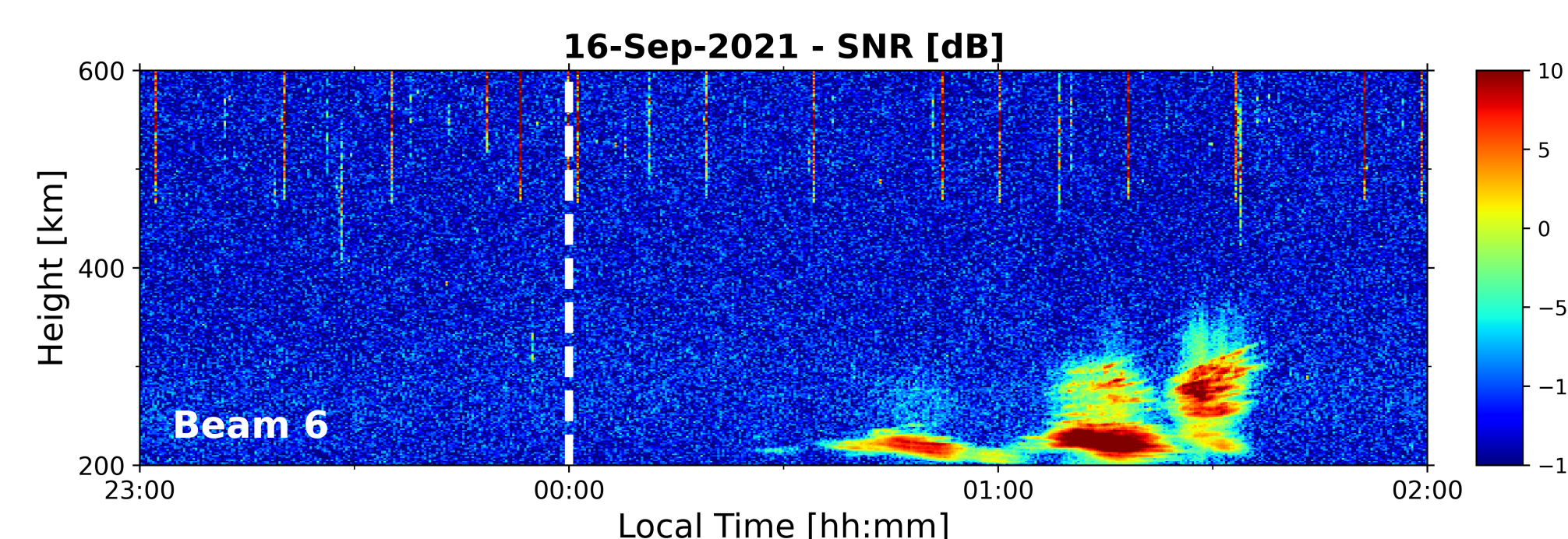


Figure 2. RTI map of UHF echoes measured by AMISR-14 beginning on 16 September 2021. Beam number is indicated in the bottom left of the panel. Please note that beam 6 corresponds to one of the AMISR-14 pointing directions closest to zenith. The white dashed line marks local midnight.

- Did the isolated post-midnight ESF event in Figure 2 form locally (i.e., within ~ 200 km to the west and to the east of the JRO), or did the observed event develop non-locally in another longitude sector before moving into the AMISR-14 FoV?

6. RESULTS AND DISCUSSION

- We created sequences of 2D “snapshots” or images of the distribution of UHF coherent backscatter echoes in the AMISR-14 FoV for the 51 nights with an isolated post-midnight ESF event.
- We then identified whether each event was associated with ESF that drifted into the wide instrument FoV already well-developed (i.e., “drifting-in” or non-local) or that generated within the FoV (i.e., “fresh” or local).
- An event was labelled local if vertically developed echoes were first measured in at least one of beams 2 through 9 (see Figure 1).
- First echoes had to be measured in beam 1 or 10, the beams pointed furthest off-zenith, for an event to be labelled as non-local.

6.1 On an example of a non-local event

- The top panel of Figure 3 shows the RTI map for beam 5 of the complete AMISR-14 observations that began the evening of 16 September 2021. The bottom panels show a sequence of 2D images.

- The sequence shows explicitly that the event generated non-locally and drifted into the instrument FoV from the west.

6.2 On an example of a local event

- Figure 4 shows an example of an event in observations that began the evening of an earlier date, 12 September 2021.
- The detection of weak and diffuse echoes in the post-midnight sector like the ones in Figure 4 would suggest the signature of so-called “fossil” ESF that formed far from the observation site.

- The sequence of 2D images shown in the bottom panels of Figure 4 reveals that the event generated locally instead, well within the AMISR-14 FoV, without detectable zonal motion.

6.3 On the occurrence rates of events

- Table 1 lists the annual and seasonal occurrence rates of both local and non-local events.
- The statistics show that (i) the highest event occurrence rate per year is in June solstice under all solar flux conditions and (ii) events occur less often in all seasons as solar flux increases.

6.1 NON-LOCAL ISOLATED POST-MIDNIGHT EQUATORIAL SPREAD F

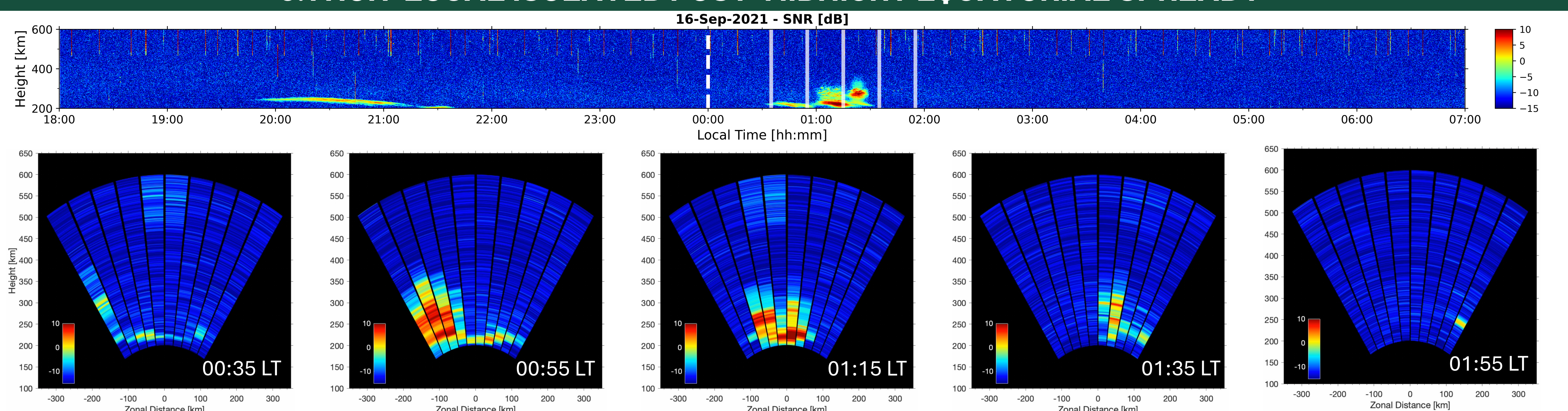


Figure 3. RTI map of UHF echoes measured by AMISR-14 beginning on 16 September 2021 (top panel). The white dashed line indicates local midnight. The transparent white solid lines mark the time of each snapshot. 2D images of the distribution of UHF echoes (bottom panels). Snapshot timestamps are also indicated in each panel.

6.2 LOCAL ISOLATED POST-MIDNIGHT EQUATORIAL SPREAD F

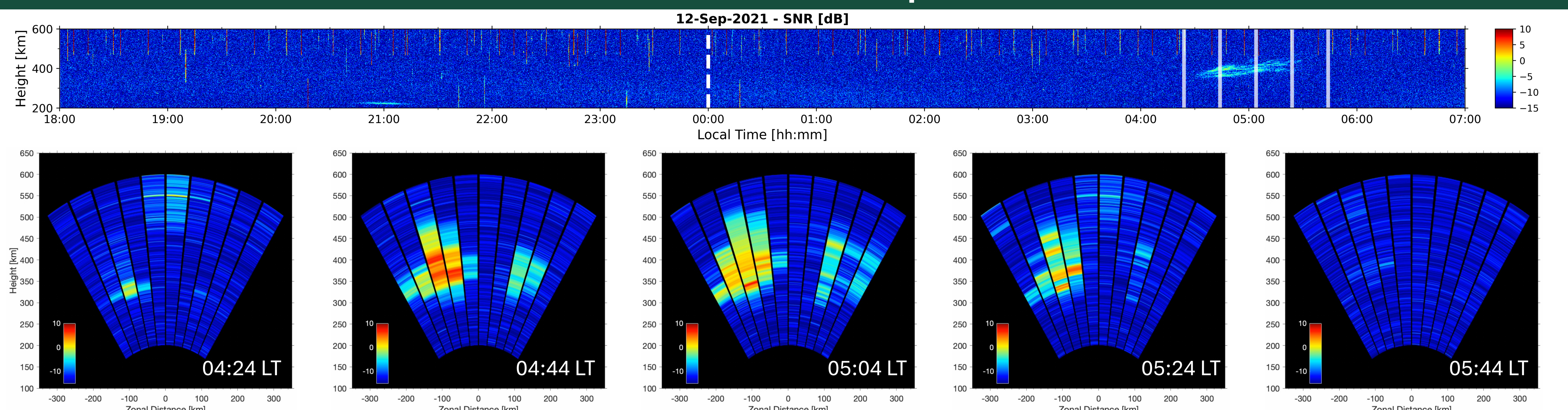


Figure 4. Beam 5 RTI map for AMISR-14 observations beginning on 12 September 2021 (top panel). The white dashed line marks local midnight. The transparent white solid lines indicate the time for each snapshot in the sequence. 2D images of the observations with all ten beams (bottom panels).

6.3 EVENT OCCURRENCE RATES

Table 1 – Number of analyzed observation nights, occurrence rates of local isolated post-midnight ESF events, occurrence rates of non-local events, and average daily F10.7 index in solar flux units organized by year and season. The final row for each year lists values for the entire analyzed period in that year. Values for geomagnetically quiet nights are indicated in parentheses where relevant.

2021				
Time period	Nights	Rate of local events	Rate of non-local events	Avg. F10.7 (SFU)
Jun. sols.	18(11)	11%(9%)	22%(18%)	81.2
Dec. sols.	51(27)	12%(11%)	8%(11%)	96.7
Equinox	43(30)	12%(7%)	7%(3%)	86.6
Analyzed period	112(68)	12%(9%)	10%(9%)	88.2
2022				
Time period	Nights	Rate of local events	Rate of non-local events	Avg. F10.7 (SFU)
Jun sols.	24(14)	13%(7%)	8%(7%)	128.1
Dec. sols.	59(24)	5%(8%)	5%(8%)	147.9
Equinox	121(41)	6%(5%)	4%(2%)	125.1
Analyzed period	204(79)	6%(6%)	5%(5%)	133.7
2023				
Time period	Nights	Rate of local events	Rate of non-local events	Avg. F10.7 (SFU)
Jun. sols.	40(14)	3%(0%)	5%(0%)	171.1
Dec. sols.	-	-	-	-
Equinox	40(11)	0%(0%)	3%(0%)	159.5
Analyzed period	80(25)	1%(0%)	4%(0%)	165.3

7. MAIN FINDINGS

- Measurements from the 10-beam AMISR-14 F-region mode have allowed us to identify the origin (i.e., local vs non-local) of isolated post-midnight ESF events.
- We found that the occurrence rate of these events decreases with solar activity. This is in good agreement with previous studies [4, 5, 6].
- Perhaps most importantly, the new 2D observations made by AMISR-14 allowed us to identify that about half of the events (27 out of 51) originated locally, that is, within ~ 200 km zonally of the JRO (SQ1).
- Additionally, the results did not show a significant effect of geomagnetic activity on the relative occurrence rates of local/non-local post-midnight events (SQ2).
- We emphasize that the distinction between local (“fresh”) and non-local (“drifting-in”) isolated post-midnight ESF events is crucial when trying to understand the conditions under which these irregularities developed based on local measurements of ionospheric and/or thermospheric parameters [e.g., 9].

ACKNOWLEDGEMENTS AND REFERENCES

This work was supported by NSF award AGS-1916055 and by the DoD through an NDSEG Fellowship. A. M. would like to thank support by UTD through a Eugene McDermott Graduate Fellowship. The JRO is a facility of the Instituto Geofísico del Perú operated with support from NSF award AGS-2213849 through Cornell University.

- Basu, B. (2002), J Geophys Res Space Physics, 107(A8).
- Rodrigues, F. S. et al. (2015), Geophys Res Lett, 42(13).
- Rodrigues, F. S. et al. (2023), Earth Planets Space, 75(120).
- Hysell, D. L. and Burcham, J. D. (2002), J Atmos Sol Terr Phys, 64(12-14).
- Smith, J. M. et al. (2016), J Geophys Res Space Physics, 121(2).
- Zhan, W. et al. (2018), Geophys Res Lett, 45(15).
- Ajith, K. K. et al. (2016), J Geophys Res Space Physics, 121(9).
- Jin, H. et al. (2021), J Geophys Res Space Physics, 126(5).
- Hysell, D. L. et al. (2018), J Geophys Res Space Physics, 123(8).